

Investigating light neutralinos at neutrino telescopes

V. Niro^{a*}, A. Bottino^{b†}, N. Fornengo^{b‡}, and S. Scopel^{c§}

^a*Max-Planck-Institut für Kernphysik,*

Postfach 103980, D-69029 Heidelberg, Germany

^b*Dipartimento di Fisica Teorica, Università di Torino*

and INFN, Sez. di Torino, via P. Giuria 1, I-10125 Torino, Italia

^c*School of Physics and Astronomy, Seoul National University*

Gwanak-ro 599, Gwangak-gu, Seoul 151-749, Korea

November 12, 2018

Abstract

We present a detailed analysis of the neutrino-induced muon signals coming from neutralino pair-annihilations inside the Sun and the Earth with particular emphasis for light neutralinos. The theoretical model considered is an effective MSSM without gaugino-mass unification, which allows neutralinos of light masses (below 50 GeV). The muon events are divided in through-going and stopping muons, using the geometry of the Super-Kamiokande detector. In the evaluation of the signals, we take into account the relevant hadronic and astrophysics uncertainties and include neutrino oscillation and propagation properties in a consistent way. We derive the ranges of neutralino masses which could be explored at neutrino telescopes with a low muon-energy threshold (around 1 GeV) depending on the category of events and on the values of the various astrophysics and particle-physics parameters. A final analysis is focussed to the upward muon fluxes which could be generated by those neutralino configurations which are able to explain the annual modulation data of the DAMA/LIBRA experiment. We show how combining these data with measurements at neutrino telescopes could help in pinning down the features of the DM particle and in restraining the ranges of the many quantities (of astrophysics and particle-physics origins) which enter in the evaluations and still suffer from large uncertainties.

*email: viviana.niro@mpi-hd.mpg.de

†email: bottino@to.infn.it

‡email: fornengo@to.infn.it

§email: scopel@phya.snu.ac.kr

1 Introduction

In the papers of Ref. [1] it was shown that light neutralinos with a mass in the range $7 \text{ GeV} \lesssim m_\chi \lesssim 50 \text{ GeV}$ are interesting candidates for particle dark matter, with direct detection rates accessible to experiments with large exposure (of order $100\,000 \text{ kg day}$) and low energy threshold (of a few keV). This population of light neutralinos arises in the Minimal Supersymmetric extension of the Standard Model (MSSM) when the unification of gaugino masses at a Grand Unified (GUT) scale is not assumed [2]. Indeed, in this supersymmetric framework the lower bound of $\sim 7 \text{ GeV}$ on the neutralino mass is set by a cosmological bound on the neutralino relic density [1]. This is at variance with the lower bound $m_\chi \gtrsim 50 \text{ GeV}$, which is derived from the LEP lower limit on the chargino mass within the MSSM with gaugino mass unification at the GUT scale.

A direct comparison of the theoretical predictions of Ref. [1] with experimental data was made possible when the DAMA Collaboration published the results of its measurements collected with a NaI detector of 100 kg over 7 annual cycles [3]. Actually, in Ref. [4] it was proved that the population of light neutralinos fitted well these DAMA results.

The inclusion of the channeling effect in the experimental analysis [5] and the further results of the DAMA/LIBRA combined data [6] confirmed the good agreement of the predictions of Ref. [1] with the experimental data, as discussed in Refs. [7, 8].

Possible indirect effects of light neutralinos were studied in Refs. [8, 9], where it was shown that present cosmic antiproton data set sizable constraints on the supersymmetric space; measurements of cosmic antideuterons [10] with forthcoming airborne experiments [11] were indicated in [8, 9] as a very promising investigation mean for the light neutralino population.

In Ref. [9] also possible signals induced in neutrino telescopes by the neutrinos produced by pair-annihilations of light neutralinos captured in the Earth and the Sun were discussed. The analysis was carried out in the case of a single category of events, those due to upward through-going muons.

In the present paper we resume the analysis of Ref. [9], by implementing and extending it in various distinctive features: a) the particle-physics uncertainties in hadronic quantities which affect the capture rate of relic neutralinos by the celestial bodies are taken into account and discussed in detail; b) all main processes that occur during the neutrino propagation: neutrino oscillations and neutrino incoherent interactions with matter are included; c) the investigation comprises also the category of upward stopping muons (actually, this turns out to be the most promising case for upward-going muons induced by pair annihilation of light neutralinos).

Indirect evidence of WIMPs in our halo by measurements of upward-going muons at neutrino telescopes, generated by WIMP pair-annihilation in celestial bodies, has been the subject of many investigations in the past, see for instance [12, 13, 14, 15].

Recently, a number of papers appeared where possible signals at neutrino telescopes due to pair annihilation of light DM particles are discussed. These consider either generic WIMPs with assumed dominance of specific annihilation channels [16, 17] or discuss specific DM candidates other than neutralinos: WIMPless dark matter and mirror dark matter

[17], leptonically interacting dark matter [18] and DM particles which directly annihilate to neutrinos [19]. All these investigations are restricted to signals from the Sun.

At variance with these analyses, the present paper deals with neutrino signals produced in cosmic macroscopic bodies by pair annihilation of light neutralinos whose specific supersymmetric properties are those which satisfy all existing particle-physics and cosmological constraints, as analyzed in Refs. [1, 8]. Furthermore, our investigation entails neutrino signals expected from the Sun as well as those from the Earth.

Our results are given first for the whole population of light neutralinos, then for those subsets which are selected by the DAMA/LIBRA results [6], when these are interpreted in terms of relic neutralinos. We separate the case where the channeling effect is included from the one where this effect is neglected.

The scheme of the present paper is the following. In Sect. 2 the main features of the supersymmetric model employed here are summarized. The formulae providing the capture rates of relic neutralinos by celestial bodies and the annihilation rates due to neutralino pair-annihilation are recalled in Sect. 3, together with some properties of the hadronic quantities which enter in the evaluations of the neutralino-nucleon cross section. The generation and the propagation of the neutrino fluxes is described in Sect. 4, their ensuing muon fluxes are derived in Sect. 5. Results and conclusions are given in Sect. 6.

2 Theoretical model

The supersymmetric scheme we employ in the present paper is the one described in Refs. [1, 8]: an effective MSSM scheme (effMSSM) at the electroweak scale, with the following independent parameters: $M_1, M_2, \mu, \tan \beta, m_A, m_{\tilde{q}}, m_{\tilde{l}}$ and A . Notations are as follows: M_1 and M_2 are the U(1) and SU(2) gaugino masses (these parameters are taken here to be positive), μ is the Higgs mixing mass parameter, $\tan \beta$ the ratio of the two Higgs v.e.v.'s, m_A the mass of the CP-odd neutral Higgs boson, $m_{\tilde{q}}$ is a squark soft-mass common to all squarks, $m_{\tilde{l}}$ is a slepton soft-mass common to all sleptons, and A is a common dimensionless trilinear parameter for the third family, $A_{\tilde{b}} = A_{\tilde{t}} \equiv Am_{\tilde{q}}$ and $A_{\tilde{\tau}} \equiv Am_{\tilde{l}}$ (the trilinear parameters for the other families being set equal to zero). In our model, no gaugino-mass unification at a Grand Unified (GUT) scale is assumed. The lightest neutralino is required to be the lightest supersymmetric particle and stable (because of R-parity conservation).

The numerical analysis presented in the present paper was performed by a scanning of the supersymmetric parameter space, with the following ranges of the MSSM parameters: $1 \leq \tan \beta \leq 50$, $100 \text{ GeV} \leq |\mu| \leq 1000 \text{ GeV}$, $5 \text{ GeV} \leq M_1 \leq 500 \text{ GeV}$, $100 \text{ GeV} \leq M_2 \leq 1000 \text{ GeV}$, $100 \text{ GeV} \leq m_{\tilde{q}}, m_{\tilde{l}} \leq 3000 \text{ GeV}$, $90 \text{ GeV} \leq m_A \leq 1000 \text{ GeV}$, $-3 \leq A \leq 3$.

The supersymmetric parameter space has been subjected to all available constraints due to accelerator data on supersymmetric and Higgs boson searches (CERN e^+e^- collider LEP2 [20] and Collider Detectors D0 and CDF at Fermilab [21]) and to other particle-physics precision results: measurements of the $b \rightarrow s + \gamma$ decay process [22] [$2.89 \leq B(b \rightarrow s + \gamma) \cdot 10^{-4} \leq 4.21$ is employed here], the upper bound on the branching ratio $BR(B_s^0 \rightarrow \mu^- + \mu^+)$ [23] [we take $BR(B_s^0 \rightarrow \mu^- + \mu^+) < 1.2 \cdot 10^{-7}$] and measurements

of the muon anomalous magnetic moment $a_\mu \equiv (g_\mu - 2)/2$: for the deviation Δa_μ of the experimental world average from the theoretical evaluation within the Standard Model we use here the range $-98 \leq \Delta a_\mu \cdot 10^{11} \leq 565$. For other details concerning these constraints see Refs. [1, 8].

Also included is the cosmological constraint that the neutralino relic abundance does not exceed the maximal allowed value for cold dark matter, *i.e.* $\Omega_\chi h^2 \leq (\Omega_{CDM} h^2)_{\max}$. We set $(\Omega_{CDM} h^2)_{\max} = 0.122$, as derived at the 2σ level from the results of Ref. [24]. We recall that this cosmological upper bound implies on the neutralino mass the lower limit $m_\chi \gtrsim 7$ GeV [1].

3 Capture rates and annihilation rates

In the present section we summarize the main formulae which we employed to evaluate the capture rates of neutralinos by celestial bodies and their pair-annihilation in neutrinos.

The capture rate C of the relic neutralinos by a macroscopic body is given by the standard formula [25]

$$C = \frac{\rho_\chi}{v_\chi} \sum_i \frac{\sigma_{\text{el},i}}{m_\chi m_i} (M_B f_i) \langle v_{\text{esc}}^2 \rangle_i X_i, \quad (1)$$

where v_χ is the neutralino mean velocity, $\sigma_{\text{el},i}$ is the cross section of the neutralino elastic scattering off the nucleus i of mass m_i , $M_B f_i$ is the total mass of the element i in the body of mass M_B , $\langle v_{\text{esc}}^2 \rangle_i$ is the square escape velocity averaged over the distribution of the element i , X_i is a factor which takes account of kinematical properties occurring in the neutralino–nucleus interactions.

The neutralino local density is denoted by ρ_χ . One can assume that ρ_χ is equal to the local value of the total DM density ρ_0 , when the neutralino relic abundance $(\Omega_\chi h^2)$ turns out to be at the level of a minimal $(\Omega_{CDM} h^2)_{\min}$ consistent with ρ_0 . On the contrary, when $(\Omega_\chi h^2)$ is smaller than $(\Omega_{CDM} h^2)_{\min}$, the value to be assigned to ρ_χ has to be appropriately reduced. Thus we evaluate $\Omega_\chi h^2$ and we determine ρ_χ by adopting a standard rescaling procedure [12]:

$$\begin{aligned} \rho_\chi &= \rho_0, & \text{when } \Omega_\chi h^2 &\geq (\Omega_{CDM} h^2)_{\min} \\ \rho_\chi &= \rho_0 \frac{\Omega_\chi h^2}{(\Omega_{CDM} h^2)_{\min}}, & \text{when } \Omega_\chi h^2 &< (\Omega_{CDM} h^2)_{\min} \end{aligned} \quad (2)$$

Here $(\Omega_{CDM} h^2)_{\min}$ is set to the value 0.098, as derived at 2σ level from the results of Ref. [24]. The neutralino relic abundance is evaluated with the procedure discussed in Ref. [1].

As for the velocity distribution of relic neutralinos in the galactic halo we use here, for definiteness, the standard isothermal distribution parametrized in terms of the local rotational velocity v_0 . It is however to be recalled that the actual distribution function could deviate sizably from the isothermal one (see, for instance, Ref. [26] for a systematic

analysis of different categories of distribution functions) or even depend on non-thermalized effects [27]. Also the possible presence of a thick disk of dark matter could play a relevant role in the capture of dark matter by celestial bodies [28]. The local rotational velocity v_0 is set at three different representative values: the central value $v_0 = 220 \text{ Km s}^{-1}$ and two extreme values $v_0 = 170 \text{ Km s}^{-1}$ and $v_0 = 270 \text{ Km s}^{-1}$ which bracket the v_0 physical range. Associated to each value of v_0 we take a value of ρ_0 within its physical range established according to the procedure described in Ref. [26]. In conclusion, we will provide the numerical results of our analysis for the following three sets of astrophysical parameters: 1) $v_0 = 170 \text{ Km s}^{-1}$, $\rho_0 = 0.20 \text{ GeV cm}^{-3}$; 2) $v_0 = 220 \text{ Km s}^{-1}$, $\rho_0 = 0.34 \text{ GeV cm}^{-3}$; 3) $v_0 = 270 \text{ Km s}^{-1}$, $\rho_0 = 0.62 \text{ GeV cm}^{-3}$. Note that these values of ρ_0 correspond to the case of maximal amount of non halo components to DM in the galaxy [26].

The annihilation rate Γ_{ANN} is expressed in terms of the capture rate by the formula [29]

$$\Gamma_{\text{ANN}} = \frac{C}{2} \tanh^2 \left(\frac{t}{\tau_A} \right), \quad (3)$$

where t is the age of the macroscopic body ($t = 4.5 \text{ Gyr}$ for Sun and Earth), $\tau_A = (CC_A)^{-1/2}$, and C_A is the annihilation rate per effective volume of the body, given by

$$C_A = \frac{\langle \sigma v \rangle}{V_0} \left(\frac{m_\chi}{20 \text{ GeV}} \right)^{3/2}. \quad (4)$$

In the above expression V_0 is defined as $V_0 = (3m_{Pl}^2 T / (2\rho \times 10 \text{ GeV}))^{3/2}$ where T and ρ are the central temperature and the central density of the celestial body. For the Earth ($T = 6000 \text{ K}$, $\rho = 13 \text{ g} \cdot \text{cm}^{-3}$) $V_0 = 2.3 \times 10^{25} \text{ cm}^3$, for the Sun ($T = 1.4 \times 10^7 \text{ K}$, $\rho = 150 \text{ g} \cdot \text{cm}^{-3}$) $V_0 = 6.6 \times 10^{28} \text{ cm}^3$. σ is the neutralino–neutralino annihilation cross section and v is the relative velocity. The thermal average $\langle \sigma v \rangle$ is calculated with all the contributions at the tree level as in Ref. [30], with the further inclusion here of the two gluon annihilation final state [13].

We recall that, according to Eq. (3), in a given macroscopic body the equilibrium between capture and annihilation (*i.e.* $\Gamma_{\text{ANN}} \sim C/2$) is established only when $t \gtrsim \tau_A$. It is worth noticing that the neutralino density ρ_χ , evaluated according to Eq. (2), enters not only in C but also in τ_A (through C). Therefore the use of a correct value for ρ_χ (rescaled according to Eq. (2), when necessary) is important also in determining whether or not the equilibrium is already set in a macroscopic body.

Explicit calculations over the whole parameter space, given in the next sections, show that, whereas for the Earth the equilibrium condition depends sensitively on the values of the model parameters, in the case of the Sun equilibrium between capture and annihilation is typically reached for the whole range of m_χ , due to the much more efficient capture rate implied by the stronger gravitational field [25].

The annihilation rate given above refers to a macroscopic body as a whole. This is certainly enough for the Sun which appears to us as a point source. On the contrary, in the case of the Earth, one has also to define an annihilation rate referred to a unit volume at point \vec{r} from the Earth center:

$$\Gamma_{\text{ANN}}(r) = \frac{1}{2} \langle \sigma v \rangle n^2(r), \quad (5)$$

where $n(r)$ is the neutralino spatial density which may be written as [29]

$$n(r) = n_0 e^{-\tilde{\alpha} m_\chi r^2}; \quad (6)$$

here $\tilde{\alpha} = 2\pi G\rho/(3T)$ and n_0 is such that

$$\Gamma_{\text{ANN}} = \frac{1}{2} \langle \sigma v \rangle \int d^3r n^2(r). \quad (7)$$

3.1 WIMP–nucleon cross section: hadronic uncertainties

In Ref. [31] it is stressed that the couplings between Higgs-bosons (or squarks) with nucleons, which typically play a crucial role in the evaluation of the neutralino-nucleus cross section, suffer of large uncertainties [32]. Actually, these couplings are conveniently expressed in terms of three hadronic quantities, *i.e.*: the pion–nucleon sigma term

$$\sigma_{\pi N} = \frac{1}{2}(m_u + m_d) \langle N | \bar{u}u + \bar{d}d | N \rangle, \quad (8)$$

the quantity σ_0 , related to the size of the SU(3) symmetry breaking,

$$\sigma_0 \equiv \frac{1}{2}(m_u + m_d) \langle N | \bar{u}u + \bar{d}d - 2\bar{s}s | N \rangle, \quad (9)$$

and the mass ratio $r = 2m_s/(m_u + m_d)$.

Because of a number of intrinsic theoretical and experimental problems, the determination of these hadronic quantities is rather poor. Conservatively, their ranges can be summarized as follows (we refer to Refs. [31, 8] for details):

$$41 \text{ MeV} \lesssim \sigma_{\pi N} \lesssim 73 \text{ MeV}, \quad (10)$$

$$\sigma_0 = 30 \div 40 \text{ MeV}, \quad (11)$$

and

$$r = 29 \pm 7. \quad (12)$$

In the present paper, in order to display the influence of the uncertainties due to the hadronic quantities on the signals at neutrino telescopes, we will report our results for three different sets of values for the quantities $(\sigma_{\pi N}, \sigma_0, r)$ as shown in Tab. 1. The set REF corresponds to the set of value referred to as *reference point* in Ref. [8]. The sets MIN and MAX listed in Tab. 1 bracket the range of hadronic uncertainties.

hadronic set	$\sigma_{\pi N}[\text{MeV}]$	$\sigma_0[\text{MeV}]$	r
MIN	41	40	25
REF	45	30	29
MAX	73	30	25

Table 1: Set of values for the hadronic quantities considered in the numerical analysis.

In the case where the neutralino-nucleus interaction is dominated by the exchange of Higgs bosons, it is straightforward to estimate by how much the capture rate C is affected by the hadronic uncertainties. Indeed, in this case the dominant term in the interaction amplitude of the neutralino-nucleus scattering is provided by coupling between the two CP-even Higgs bosons and the down-type quarks:

$$g_d = \frac{2}{27} \left(m_N + \frac{23}{4} \sigma_{\pi N} + \frac{23}{5} r (\sigma_{\pi N} - \sigma_0) \right), \quad (13)$$

where m_N is the nucleon mass. Then:

$$C_{\text{MIN}}/C_{\text{REF}} \simeq (g_{d,\text{MIN}}/g_{d,\text{REF}})^2, \quad C_{\text{MAX}}/C_{\text{REF}} \simeq (g_{d,\text{MAX}}/g_{d,\text{REF}})^2. \quad (14)$$

Using the values of Table 1 for the three sets of hadronic quantities, one finds for g_d : $g_{d,\text{MIN}} = 99$ MeV, $g_{d,\text{REF}} = 290$ MeV, $g_{d,\text{MAX}} = 598$ MeV, respectively. We thus conclude that, because of the hadronic uncertainties, the capture rate in the case of set MIN is reduced by a factor ~ 9 as compared to the capture rate evaluated with the set REF, whereas C , evaluated with set MAX, is enhanced by a factor ~ 4 .

The consequences over the annihilation rate Γ_{ANN} is more involved, since the capture rate C enters in Γ_{ANN} not only linearly but also through τ_A . When in the celestial body capture and annihilation are in equilibrium ($t \gtrsim \tau_A$), one has $\Gamma_{\text{ANN}} \sim C/2$; then Γ_{ANN} , as a function of the hadronic quantities, rescales as C (see Eq. (14)); however, when the equilibrium is not realized, the uncertainties in Γ_{ANN} can be much more pronounced. For instance, for $t \ll \tau_A$, Γ_{ANN} is proportional to C^2 , thus the rescaling factors for Γ_{ANN} are the squares of those in Eq. (14).

These estimates will be confirmed by the numerical analysis displayed in the following section.

3.2 Numerical evaluations

The left panel of Fig. 1 shows the scatter plots for the ratios of the capture rates $C_i^{\text{Earth}}/C_{\text{REF}}^{\text{Earth}}$ (where $i = \text{set MIN, set MAX}$), obtained with the scanning of the parameter space illustrated in Sect. 2. One sees that, as anticipated in the previous section, the numerical values accumulate (most significantly for light masses), around the numerical factors shown in Eq. (14).

The scatter plots for the ratios $\Gamma_{\text{ANN},i}^{\text{Earth}}/\Gamma_{\text{ANN,REF}}^{\text{Earth}}$ (where $i = \text{set MIN, set MAX}$) are displayed in the right panel of Fig. 1. As expected and discussed before, these numerical values are much larger as compared to those of the ratios $C_i^{\text{Earth}}/C_{\text{REF}}^{\text{Earth}}$, since many supersymmetric configurations are not able to provide a capture-annihilation equilibrium inside the Earth. This interpretation is validated by the scatter plots of Fig. 2, where one sees that for most configurations the equilibrium factor $\tanh^2(t_0/\tau_A)$ deviate largely from the equilibrium value $\tanh^2(t_0/\tau_A) = 1$.

The dependence of the annihilation rate for the Sun, $\Gamma_{\text{ANN}}^{\text{Sun}}$ on the hadronic uncertainties is shown in Fig. 3. Since the capture-annihilation equilibrium is realized in the Sun for all supersymmetric configurations of our model, one has here that $\Gamma_{\text{ANN},i}^{\text{Sun}}/\Gamma_{\text{ANN,REF}}^{\text{Sun}} = C_i^{\text{Sun}}/C_{\text{REF}}^{\text{Sun}}$, which implies that $\Gamma_{\text{ANN,MAX}}^{\text{Sun}}/\Gamma_{\text{ANN,REF}}^{\text{Sun}} \lesssim 4$ and $\Gamma_{\text{ANN,MIN}}^{\text{Sun}}/\Gamma_{\text{ANN,REF}}^{\text{Sun}} \gtrsim 1/9$. This is at variance with the case of the Earth which we have commented before.

Moreover, one notices from Fig. 3 that for many supersymmetric configurations $\Gamma_{\text{ANN}}^{\text{Sun}}$ depends very slightly (or negligibly) on the variations in the the hadronic quantities. This is due to the fact that on many instances the capture of neutralinos from the Sun is dominated by spin-dependent cross-sections.

4 Calculation of neutrino fluxes

4.1 Neutrino production

Once the Dark Matter particles are accumulated in the center of the Sun and the Earth, they can annihilate into leptons, quarks, gauge and higgs bosons. These particles then decay producing neutrinos. To calculate the neutrino spectra coming from each annihilation channel, lepton decay and quark hadronization process have to be considered. In [33], the authors have used a PYTHIA Monte Carlo simulation to calculate the spectra of neutrinos, coming from Dark Matter annihilation in the Sun and in the Earth, for the following channels: $b\bar{b}$, $\tau\bar{\tau}$, $c\bar{c}$, $q\bar{q}$, gg (with $q = u, d, s$ quarks). Three main differences and improvements have been implemented in [33] with respect to previous calculations. The first one is the prediction of the neutrino spectra for the different neutrino flavors: ν_e , ν_μ and ν_τ (not only ν_μ , like in previous works). The second main improvement consists in an appropriate implementation of the energy loss that hadrons and leptons can undergo before decaying. Finally, the third difference is represented by the calculation of the neutrino spectra for light quarks u, d, s , that were usually neglected in previous calculations.

We use the initial neutrino spectra reported in [33] for $b\bar{b}$, $\tau\bar{\tau}$, $c\bar{c}$, $q\bar{q}$ and gg annihilation channels. The annihilation of two neutralinos can also produce two higgs bosons or one gauge and one higgs boson in the final state, although these two channels (as well as the annihilation channels into $t\bar{t}$ and into two gauge bosons) are absent for $m_\chi \leq 80$ GeV (we remind that our model has an absolute lower limit on the higgs mass of 90 GeV).

4.2 Neutrino propagation

For a precise estimate of the neutrino flux at the detector site, it is important to take into account the main processes that can occur during the neutrino propagation: the oscillation and the incoherent interaction with matter. These effects have been vastly analyzed in [33, 34], and then applied to specific model-dependent studies, see e.g. [35].

The equations that describe the evolution of the neutrino spectra can be formally written using the density matrix formalism:

$$\frac{d\rho}{dr} = -i[H, \rho] + \left. \frac{d\rho}{dr} \right|_{NC} + \left. \frac{d\rho}{dr} \right|_{CC}. \quad (15)$$

The first term describes the oscillation of neutrinos in matter, where the Hamiltonian is given by the sum of the mass matrix in the weak basis $(\nu_e, \nu_\mu, \nu_\tau)$ and the Wolfenstein potential:

$$H_w = \frac{M_w}{2E} \pm \sqrt{2} G_F N_e \text{diag}(1, 0, 0) \quad (16)$$

holds for (anti-)neutrinos for the minus (plus) sign. We fix the values for the neutrino mixing angles and squared mass differences to the best fit values reported in [36], and we set the mixing angle θ_{13} to zero. A different choice of θ_{13} would marginally affect the prediction on the neutrino flux, as reported in [33, 34].

The second term in Eq. (15) takes into account the neutrino energy loss and the re-injection due to neutral current interactions. The last term, instead, represents the neutrino absorption and ν_τ regeneration through charge current interactions. For the explicit form of each term and for exhaustive explanations we refer to [33].

For Dark Matter annihilation inside the Sun, the integro-differential equation for the density matrix has to be solved numerically to find the neutrino spectra at the detector site. For simplicity, we neglect the ν_τ regeneration effect, since it provides only a negligible correction for the WIMPs mass range of our interest: $m_\chi \leq 80$ GeV.

In the case of annihilations inside the Earth’s core, the calculation of the neutrino spectra can be further simplified. Indeed, the interactions with matter can be neglected, since the mean free paths of neutrinos, in the core and in the mantle, are much bigger than the Earth’s radius R_\oplus for $E_\nu \lesssim 10$ TeV (for anti-neutrinos the mean free paths are almost a factor two greater, due to the difference in the cross-sections):

$$\lambda^{core} = \frac{1}{\sigma_\nu N_e^{core}} \simeq 3.6 \times 10^4 \frac{R_\oplus}{(E_\nu/\text{GeV})}, \quad \lambda^{mantle} = \frac{1}{\sigma_\nu N_e^{mantle}} \simeq 9.2 \times 10^4 \frac{R_\oplus}{(E_\nu/\text{GeV})}. \quad (17)$$

Therefore, for the propagation inside the Earth, it can be safely taken into account only the oscillation effect. Moreover, for $E_\nu \gtrsim 1$ GeV, the dependence on the “solar” parameters Δm_{21}^2 and θ_{12} is extremely weak and can be neglected. Since we are considering vanishing θ_{13} , Earth’s matter effects are negligible and the neutrino oscillation is driven by the “atmospheric” parameters Δm_{31}^2 and θ_{23} . In this case, the main oscillation channel is the

$\nu_\mu \leftrightarrow \nu_\tau$ and the value of the oscillation and the survival probability $P_{\alpha\beta}$ is simply given by the vacuum two-flavors formula:

$$P_{\alpha\beta}(r, E_\nu) = \delta_{\alpha\beta} - \epsilon_{\alpha\beta} \sin^2(2\theta) \sin^2 \left(1.27 \frac{(\Delta m_{31}^2/eV^2)(r/\text{km})}{(E_\nu/\text{GeV})} \right), \quad (18)$$

where the parameter $\epsilon_{\alpha\beta}$ is equal to 1 (-1) for $\alpha = \beta$ ($\alpha \neq \beta$).

In the case of the Earth, the differential muon-neutrino flux at the detector, as a function of the zenith angle θ_z , can be written as:

$$\frac{dN_{\nu_\mu}}{dE_\nu d \cos \theta_z} = \frac{\Gamma_{\text{ANN}}}{4\pi R_\oplus^2} \sum_f BR_f \left(G_{\mu\mu}(\theta_z, E_\nu) \frac{dN_f^{\nu_\mu}}{dE_\nu} + G_{\mu\tau}(\theta_z, E_\nu) \frac{dN_f^{\nu_\tau}}{dE_\nu} \right), \quad (19)$$

where the function $G_{\alpha\beta}(\theta_z, E_\nu)$ encodes the dependence on the oscillation probability and on the WIMP distribution inside the Earth. Using Eq. (6), we find the following expression:

$$G_{\alpha\beta}(\theta_z, E_\nu) = \frac{2(2m_\chi \tilde{\beta})^{3/2}}{\pi^{1/2} R_\oplus} \int_0^y dr \exp[-2m_\chi \tilde{\alpha}(r^2 + R_\oplus^2 - ry)] P_{\alpha\beta}(r, E_\nu), \quad (20)$$

with $y \equiv 2R_\oplus \cos \theta_n$, $\theta_n \equiv \pi - \theta_z$ and $\tilde{\beta} = \tilde{\alpha} R_\oplus^2$. The differential muon anti-neutrino flux at the detector can be obtained by a formula analogous to Eq. (19).

5 Muon fluxes

For the calculation of up-going muons we follow the formalism described in [37], to which we refer for specific details. In these references, it has been shown that the differential muon flux is given by the following expression:

$$\frac{dN_\mu}{d \cos \theta_z dE_\mu} = N_A \frac{1}{a + bE_\mu} \int_{E_\mu}^\infty dE_\nu \int_{E_\mu}^{E_\nu} dE'_\mu \frac{dN_{\nu_\mu}}{d \cos \theta_z dE_\nu} \frac{d\sigma_{\nu_\mu}(E_\nu, E'_\mu)}{dE'_\mu}. \quad (21)$$

The quantities a and b parametrize the energy loss due to ionization and to radiative effects, N_A is the Avogadro's number and $d\sigma_{\nu_\mu}/dE'_\mu$ is the differential charge current cross section, which is mainly due to deep inelastic scattering, for energies $E_\nu > 1$ GeV. The total muon flux is then divided in through-going and stopping muons:

$$\Phi_\mu^{S,T}(\cos \theta_z) = \frac{1}{A(L_{min}, \theta_z)} \int_{E_\mu^{th}}^\infty dE_\mu \frac{dN_\mu}{d \cos \theta_z dE_\mu} A^{S,T}(L(E_\mu), \theta_z), \quad (22)$$

with E_μ^{th} being the energy threshold of the detector for upward-going muons, L the muon range in water ($L = \frac{1}{b} \ln \frac{a+bE_\mu}{a+b m_\mu}$) and $L_{min} \equiv L(E_\mu^{th})$. The function $A^{S,T}(L, \theta_z)$ represents the effective area for through-going and stopping muons, while, $A(L_{min}, \theta_z)$ is the total effective area of the detector, i.e. the projected area that corresponds to internal path-lengths longer than L_{min} , for a fixed value of the zenith angle θ_z .

The classification of upward-going muons into the two subcategories reported above is strictly detector-dependent, since it depends on the shape and the size of the detector. For a detector with cylindrical geometry (with radius R and height H), it has been shown in [38] that the function $A(L, \theta_z)$ acquires the form:

$$A(L, \theta_z) = 2RH \sin \theta_z \sqrt{1 - x^2} + 2R^2 |\cos \theta_z| \left[\cos^{-1} x - 3x \sqrt{1 - x^2} \right] \Theta(L_{max}(\theta_z) - L), \quad (23)$$

with $x = L \sin \theta_z / 2R$ and $L_{max}(\theta_z) = \min[2R / \sin \theta_z, H / |\cos \theta_z|]$. The effective area for stopping muons $A^S(L, \theta_z)$ is given by Eq. (23) and the one for through-going is $A^T(L, \theta_z) \equiv [A(L_{min}, \theta_z) - A(L, \theta_z)]$.

We will focus our analysis to the SK detector. Indeed, even if the recent results of Ice-Cube 22-strings [39] improve the SK bound in the high mass region ($m_\chi \gtrsim 200$ GeV for the hard channel and $m_\chi \gtrsim 500$ GeV for the soft channel), they do not constrain the parameter space at low masses. The Ice-Cube detector, provided with the Deep-Core arrays [40], will improve significantly the SK bound for mass $m_\chi \gtrsim 40$ GeV, as has been shown in [41], but not for the low mass range in which we are mainly interested: $7 \text{ GeV} \leq m_\chi \leq 80 \text{ GeV}$.

The SK detector has $R = 16.9$ m, $H = 36.2$ m and an energy threshold $E_\mu^{th} = 1.6$ GeV (that corresponds to $L_{min} = 7$ m). Using these features the effective area can be calculated through Eq. (23) and, with Eq. (22), the muons coming from Dark Matter annihilation can be divided in through-going and stopping muons. The same formalism can be applied to the calculation of the expected muons background coming from atmospheric neutrinos. We use the atmospheric neutrino flux from Honda et al. [42] and we reproduce with great accuracy the zenith angle distribution for stopping and through-going muons, as predicted by the SK collaboration. For the muon energy loss in rock and in water, we use the tabulated values reported in [43]. Following the analysis for through-going muons of [44], the SK limit on the muon flux can be defined as:

$$\Phi(\theta_z; 90\% \text{ C.L.}) = \frac{N_{90}}{A(L_{min}, \theta_z) \times T}, \quad (24)$$

where N_{90} is the upper Poissonian limit at the 90% C.L., given the measured events and the muons background from atmospheric neutrino, and T is the detector lifetime. We do not consider the detector efficiency, since it is almost equal to 100% for upward-going muons. Using Eq. (24) and the SK data collected from May 1996 to July 2001 [45], we find the following limits on through-going (Φ_μ^T) and stopping (Φ_μ^S) muons:

$$\Phi_{\mu, Earth}^T \lesssim 0.8 \times 10^{-14} \text{ cm}^{-2} \text{ s}^{-1} \quad \text{at } 90\% \text{ C.L.}, \quad (25)$$

$$\Phi_{\mu, Earth}^S \lesssim 0.5 \times 10^{-14} \text{ cm}^{-2} \text{ s}^{-1} \quad \text{at } 90\% \text{ C.L.}, \quad (26)$$

$$\Phi_{\mu, Sun}^T \lesssim 1.2 \times 10^{-14} \text{ cm}^{-2} \text{ s}^{-1} \quad \text{at } 90\% \text{ C.L.}, \quad (27)$$

$$\Phi_{\mu, Sun}^S \lesssim 0.5 \times 10^{-14} \text{ cm}^{-2} \text{ s}^{-1} \quad \text{at } 90\% \text{ C.L.}, \quad (28)$$

The limits for the Earth are obtained considering the angular bin $-1.0 \leq \cos \theta_z \leq -0.9$, while the values reported for the Sun are the average limits obtained varying the zenith angle from $\cos \theta_z = -1.0$ to $\cos \theta_z = 0$.

The values reported in Eqs. (25)÷(28) have to be compared with the muon flux induced by neutralinos annihilation. For the case of the Earth, we fix the angular opening to $-1.0 \leq \cos \theta_z \leq -0.9$ also for the calculation of muons coming from Dark Matter. For the case of the Sun, we divide the muons in stopping and through-going using the SK effective area averaged over the zenith angle.

In the calculation of the muon flux, we neglect the kinematical angle between the neutrino and muon direction, which can be relatively large for muons close to threshold. In any case, the average deflection angle is at most of the same order of the angular bin over which we integrate our signal, for the stopping and through going muons. Considering also the detector resolution, to neglect the kinematical angle does not affect our results in a relevant way. This is confirmed by the quite good agreement we obtain in our calculation of the atmospheric-neutrino events with the SK evaluation [46].

6 Results and conclusions

In this section we give our results for the muon fluxes expected at a neutrino telescope with a threshold muon energy of 1.6 GeV, generated by annihilation of light neutralino pair-annihilation in the Earth and in the Sun.

6.1 Fluxes from the Earth

The upper panel of Fig. 4 displays the scatter plots for the expected muon flux integrated over the muon energy for $E_\mu \geq 1.6$ GeV for the upward through-going muons. The three columns refer to the evaluation of the fluxes using in turn the three different set of hadronic quantities defined in Sect. 3.1.

The main features common to the three scatter plots are easily interpretable in terms of the following properties:

i) The various peaks for $m_\chi \lesssim 40$ GeV are due to resonant capture of neutralinos on oxygen, silicon and magnesium; indeed, these elements are almost as abundant in Earth as iron, which is the most relevant target nucleus for the capture of neutralinos of higher mass. The dip at $m_\chi \sim 45$ GeV is a consequence of a depletion of the neutralino local density, implied by the rescaling recipe of Eq. (2) and a resonant effect in the (Z-exchange) neutralino pair annihilation when $m_\chi \lesssim m_Z/2$ (note that the neutralino relic abundance is inversely proportional to the neutralino pair-annihilation).

ii) Also the fact that the muon signal for light neutralinos ($m_\chi \lesssim 25$ -30 GeV) is lower than the one at higher masses can be understood. Indeed, for light neutralino masses the branching ratio of the annihilation process into the $\tau - \bar{\tau}$ final state, which is the one with the highest neutrino yield per annihilation, is suppressed. This last property being in turn due to the fact that, for these masses, the final state in $b - \bar{b}$ in the annihilation cross

section has to be the dominant one in order to keep the neutralino relic abundance below its cosmological upper bound [1].

iii) Moreover, lower m_χ masses imply softer neutrino spectra which entail fewer muons above threshold.

The comparison of the fluxes in the three columns shows how relevant can be the role of the size of the hadronic quantities on the final outputs. The suppression (enhancement) of the flux in the case of the set MIN (MAX) as compared to the flux for the set REF are set by the numerical factors previously discussed for $\Gamma_{\text{ANN}}^{\text{Earth}}$. This entails that, whereas the overall muon flux is completely below the present experimental bound in the case of the minimal set of the hadronic quantities, some part of the spectrum would emerge sizably above the limit for neutralino masses $m_\chi \gtrsim 50$ GeV for the other sets. In the case of set MAX, neutralino configurations with masses $m_\chi \sim 15$ GeV or $m_\chi \sim 25\text{-}30$ GeV might produce some measurable signal.

Since also the dependence of the muon signals on the astrophysical parameters v_0 and ρ_0 is important, in the lower panel of Fig. 4 we display the through-going fluxes for the three representative values of v_0 and ρ_0 which we discussed in Sect. 3. The overall increase in the fluxes in moving from left to right is essentially due to the increase in the value of the local DM density. In these scatter plots the hadronic quantities are set to the value REF.

The fluxes for upward stopping-muons from the Earth are given in Fig. 5. The scheme of this figure is the same as the one of the previous Fig. 4: the dependence of the fluxes on the hadronic quantities can be read in the upper panel, the one on the astrophysical parameters is displayed in the lower panel.

Because of the uncertainties affecting the evaluations of the muon fluxes, mainly due to the hadronic quantities, we cannot convert these results in terms of absolute constraints on supersymmetric configurations. However, we can conclude that the analysis of stopping muons from the Earth can have an interesting discovery potential not only for masses above 50 GeV, but also for light neutralinos with $m_\chi \sim 15$ GeV or $m_\chi \sim 25\text{-}30$ GeV. Notice however that the neutralino configurations which provide the highest values of the muon fluxes, mainly at $m_\chi \sim 50\text{-}70$ GeV, are actually disfavored by measurements of WIMP direct detection [47] which have their maximal sensitivity in this mass range.

6.2 Fluxes from the Sun

The fluxes of upward through-going muons and for stopping muons from the Sun are provided in Fig. 6 and in Fig. 7, respectively. The schemes of these figures is the same as the ones of the previous Fig. 4 and Fig. 5, respectively: the dependence of the fluxes on the hadronic quantities can be read in the upper panels of Fig. 6 and Fig. 7, the one on the astrophysical parameters is displayed in the lower panels of the same figures.

From these results one notices that through-going muons can only be relevant for neutralinos with masses $m_\chi \gtrsim 50$ GeV or $m_\chi \sim 35\text{-}40$ GeV, whereas stopping muons can potentially provide information also on some supersymmetric configurations with masses

down to $m_\chi \sim 7$ GeV, in the favorable cases of high values of the hadronic quantities and of the astrophysical parameters.

6.3 Fluxes of stopping muons for supersymmetric configurations selected by the DAMA/LIBRA annual modulation data

Now we give the expected upward muon fluxes from Earth and Sun which would be produced by neutralino configurations which fit the annual modulation data of the DAMA/LIBRA experiment [6]. As before, for definiteness the analysis is performed in the framework of the isothermal sphere. The selection of the supersymmetric configurations is performed on the basis of the analysis carried out in Ref. [8]: for any set of astrophysical parameters and hadronic quantities, from the whole neutralino population are extracted the configurations which fit the experimental annual modulation data, and the relevant muon fluxes are evaluated. As for the yearly modulation data, we consider both outputs of the experimental analysis of the DAMA Collaboration: those where the channelling effect [5] is included as well as those where this effect is neglected. We recall that the way by which the channeling effect has to be taken into account in the analysis is still under study; thus the actual physical outputs in the analysis of the experimental data in terms of specific DM candidates could stay mid-way, between the case defined as channeling and the no-channeling one, respectively.

We only report the results for stopping muons, since, as we have seen above, this is the category of events which can provide the most sizable signals. To avoid proliferation of figures, only fluxes calculated with the set REF for the hadronic quantities is reported here.

Fig. 8 displays the fluxes for the upward stopping muons expected from the Earth in case of no-channeling (upper panel) and in the case of channeling (lower panel). The corresponding fluxes from the Sun are shown in Fig. 9.

We note that depending on the role of channeling in the extraction of the physical supersymmetric configurations, the stopping muon fluxes can have a discovery potential with an interesting complementarity between the signals from the two celestial bodies: whereas the flux from the Earth cannot give insights into neutralino masses below about 15 GeV, the flux from the Sun would potentially be able to measure effects down to $m_\chi \sim 7$ GeV.

It is worth remarking that under favorable conditions provided by the actual values of the involved parameters, a combination of the annual modulation data and of measurements at neutrino telescopes could help in pinning down the features of the DM particle and in restraining the ranges of the many quantities (of astrophysical and particle-physics origins) which enter in the evaluations and still suffer from large uncertainties.

We stress once more that the present analysis, for definiteness, was performed only in the standard case of a halo DM distribution function given by an isothermal sphere. Use of different halo distributions such as those mentioned in Sect. 3 could modify sizably the role of specific supersymmetric configurations.

We wish here to recall that indirect signals of light neutralinos could also be provided by future measurements of cosmic antideuterons in space [10]. Finally, investigations at the Large Hadron Collider will hopefully provide a crucial test bench for the very existence of these light supersymmetric stable particles [48].

Acknowledgments

We acknowledge Research Grants funded jointly by Ministero dell’Istruzione, dell’Università e della Ricerca, by Università di Torino and by Istituto Nazionale di Fisica Nucleare within the *Astroparticle Physics Project*. S. S. acknowledges support of the WCU program (R32-2008-000-10155-0) of the National Research Foundation of Korea.

References

- [1] A. Bottino, N. Fornengo, and S. Scopel, *Light relic neutralinos*, *Phys. Rev.* **D67** (2003) 063519, [[hep-ph/0212379](#)]; A. Bottino, F. Donato, N. Fornengo, and S. Scopel, *Lower bound on the neutralino mass from new data on CMB and implications for relic neutralinos*, *Phys. Rev.* **D68** (2003) 043506, [[hep-ph/0304080](#)].
- [2] Specific supersymmetric models which generate light neutralinos can be envisaged; for a very recent realization of the light neutralino scenario see for instance E. Dudas, S. Lavignac, and J. Parmentier, *A light neutralino in hybrid models of supersymmetry breaking*, *Nucl. Phys.* **B808** (2009) 237–259, [[arXiv:0808.0562](#)].
- [3] R. Bernabei *et. al.*, *Dark matter search*, *Riv. Nuovo Cim.* **26N1** (2003) 1–73, [[astro-ph/0307403](#)].
- [4] A. Bottino, F. Donato, N. Fornengo, and S. Scopel, *Light neutralinos and WIMP direct searches*, *Phys. Rev.* **D69** (2004) 037302, [[hep-ph/0307303](#)].
- [5] R. Bernabei *et. al.*, *Possible implications of the channeling effect in NaI(Tl) crystals*, *Eur. Phys. J.* **C53** (2008) 205–213, [[arXiv:0710.0288](#)].
- [6] R. Bernabei *et. al.*, *First results from DAMA/LIBRA and the combined results with DAMA/NaI*, *Eur. Phys. J.* **C56** (2008) 333–355, [[arXiv:0804.2741](#)].
- [7] A. Bottino, F. Donato, N. Fornengo, and S. Scopel, *Zooming in on light relic neutralinos by direct detection and measurements of galactic antimatter*, *Phys. Rev.* **D77** (2008) 015002, [[arXiv:0710.0553](#)].
- [8] A. Bottino, F. Donato, N. Fornengo, and S. Scopel, *Interpreting the recent results on direct search for dark matter particles in terms of relic neutralino*, *Phys. Rev.* **D78** (2008) 083520, [[arXiv:0806.4099](#)].

- [9] A. Bottino, F. Donato, N. Fornengo, and S. Scopel, *Indirect signals from light neutralinos in supersymmetric models without gaugino mass unification*, *Phys. Rev.* **D70** (2004) 015005, [[hep-ph/0401186](#)].
- [10] F. Donato, N. Fornengo, and P. Salati, *Antideuterons as a signature of supersymmetric dark matter*, *Phys. Rev.* **D62** (2000) 043003, [[hep-ph/9904481](#)]; F. Donato, N. Fornengo, and D. Maurin, *Antideuteron fluxes from dark matter annihilation in diffusion models*, *Phys. Rev.* **D78** (2008) 043506, [[arXiv:0803.2640](#)]; H. Baer and S. Profumo, *Low energy antideuterons: Shedding light on dark matter*, *JCAP* **0512** (2005) 008, [[astro-ph/0510722](#)].
- [11] C. J. Hailey *et. al.*, *Accelerator testing of the General Antiparticle Spectrometer, a novel approach to indirect dark matter detection*, *JCAP* **0601** (2006) 007, [[astro-ph/0509587](#)]; J. Koglin, *Talk at “The Hunt for Dark Matter”*, Fermilab (May 10-12, 2007); V. Choutko and F. Giovacchini, *on behalf of the AMS Collaboration, Proceedings of the 30th International Cosmic Ray Conference*, Merida (Mexico) (2007).
- [12] T. K. Gaisser, G. Steigman, and S. Tilav, *Limits on Cold Dark Matter Candidates from Deep Underground Detectors*, *Phys. Rev.* **D34** (1986) 2206.
- [13] M. Drees, G. Jungman, M. Kamionkowski, and M. M. Nojiri, *Neutralino annihilation into gluons*, *Phys. Rev.* **D49** (1994) 636–647, [[hep-ph/9306325](#)].
- [14] J. Silk, K. A. Olive, and M. Srednicki, *The photino, the sun, and high-energy neutrinos*, *Phys. Rev. Lett.* **55** (1985) 257–259; K. Freese, *Can Scalar Neutrinos Or Massive Dirac Neutrinos Be the Missing Mass?*, *Phys. Lett.* **B167** (1986) 295; G. F. Giudice and E. Roulet, *Energetic neutrinos from supersymmetric Dark Matter*, *Nucl. Phys.* **B316** (1989) 429; G. B. Gelmini, P. Gondolo, and E. Roulet, *Neutralino dark matter searches*, *Nucl. Phys.* **B351** (1991) 623–644; M. Kamionkowski, *Energetic neutrinos from heavy neutralino annihilation in the sun*, *Phys. Rev.* **D44** (1991) 3021–3042; F. Halzen, T. Stelzer, and M. Kamionkowski, *Signatures of dark matter in underground detectors*, *Phys. Rev.* **D45** (1992) 4439–4442; M. Mori *et. al.*, *Search for neutralino dark matter in Kamiokande*, *Phys. Rev.* **D48** (1993) 5505–5518; R. Gandhi, J. L. Lopez, D. V. Nanopoulos, K.-j. Yuan, and A. Zichichi, *Scrutinizing supergravity models through neutrino telescopes*, *Phys. Rev.* **D49** (1994) 3691–3703, [[astro-ph/9309048](#)]; L. Bergstrom, J. Edsjo, and P. Gondolo, *Indirect neutralino detection rates in neutrino telescopes*, *Phys. Rev.* **D55** (1997) 1765–1770, [[hep-ph/9607237](#)]; L. Bergstrom, J. Edsjo, and M. Kamionkowski, *Astrophysical-neutrino detection with angular and energy resolution*, *Astropart. Phys.* **7** (1997) 147–160, [[astro-ph/9702037](#)].
- [15] A. Bottino, V. de Alfaro, N. Fornengo, G. Mignola, and M. Pignone, *Indirect search for neutralinos at neutrino telescopes*, *Phys. Lett.* **B265** (1991) 57–63; A. Bottino, N. Fornengo, G. Mignola, and L. Moscoso, *Signals of neutralino dark matter from earth and sun*, *Astropart. Phys.* **3** (1995) 65–76, [[hep-ph/9408391](#)]; V. Berezhinsky *et. al.*, *Searching for relic neutralinos using neutrino telescopes*, *Astropart. Phys.* **5** (1996) 333–352,

- [[hep-ph/9603342](#)]; A. Bottino, F. Donato, N. Fornengo, and S. Scopel, *Combining the data of annual modulation effect in WIMP direct detection with measurements of WIMP indirect searches*, *Astropart. Phys.* **10** (1999) 203–210, [[hep-ph/9809239](#)]; A. Bottino, F. Donato, N. Fornengo, and S. Scopel, *Further investigation of a relic neutralino as a possible origin of an annual-modulation effect in WIMP direct search*, *Phys. Rev.* **D62** (2000) 056006, [[hep-ph/0001309](#)].
- [16] D. Hooper, F. Petriello, K. M. Zurek, and M. Kamionkowski, *The New DAMA Dark-Matter Window and Energetic-Neutrino Searches*, *Phys. Rev.* **D79** (2009) 015010, [[arXiv:0808.2464](#)].
- [17] J. L. Feng, J. Kumar, J. Learned, and L. E. Strigari, *Testing the Dark Matter Interpretation of the DAMA/LIBRA Result with Super-Kamiokande*, [arXiv:0808.4151](#).
- [18] J. Kopp, V. Niro, T. Schwetz, and J. Zupan, *DAMA/LIBRA and leptonically interacting Dark Matter*, [arXiv:0907.3159](#).
- [19] J. Kumar, J. G. Learned, and S. Smith, *Light Dark Matter Detection Prospects at Neutrino Experiments*, [arXiv:0908.1768](#).
- [20] A. Colaleo (ALEPH Collaboration), talk at SUSY'01, June 11-17, 2001, Dubna, Russia; J. Abdallah et al. (DELPHI Collaboration), DELPHI 2001-085 CONF 513, June 2001.; LEP Higgs Working Group for Higgs boson searches, *Search for the standard model Higgs boson at LEP*, [hep-ex/0107029](#); L. (<http://lepsusy.web.cern.ch/lepsusy/>).
- [21] A. A. Affolder *et al.*, *Search for neutral supersymmetric Higgs bosons in $p\bar{p}$ collisions at $\sqrt{s} = 1.8$ TeV*, *Phys. Rev. Lett.* **86** (2001) 4472–4478, [[hep-ex/0010052](#)]; V. M. Abazov *et al.*, *Search for pair production of scalar bottom quarks in $p\bar{p}$ collisions at $\sqrt{s} = 1.96$ -TeV*, *Phys. Rev. Lett.* **97** (2006) 171806, [[hep-ex/0608013](#)].
- [22] E. Barberio *et al.*, *Averages of b -hadron properties at the end of 2005*, [hep-ex/0603003](#).
- [23] V. M. Abazov *et al.*, *Search for $B_s \rightarrow \mu^+\mu^-$ at D0*, *Phys. Rev.* **D76** (2007) 092001, [[arXiv:0707.3997](#)].
- [24] J. Dunkley *et al.*, *Five-Year Wilkinson Microwave Anisotropy Probe (WMAP) Observations: Likelihoods and Parameters from the WMAP data*, *Astrophys. J. Suppl.* **180** (2009) 306–329, [[arXiv:0803.0586](#)].
- [25] A. Gould, *Resonant Enhancements in WIMP Capture by the Earth*, *Astrophys. J.* **321** (1987) 571; A. Gould, *Direct and indirect capture of WIMPs by the Earth*, *Astrophys. J.* **328** (1988) 919–939; A. Gould, *Gravitational diffusion of solar system WIMPs*, *Astrophys. J.* **368** (Feb., 1991) 610–615.

- [26] P. Belli, R. Cerulli, N. Fornengo, and S. Scopel, *Effect of the galactic halo modeling on the DAMA/NaI annual modulation result: an extended analysis of the data for WIMPs with a purely spin-independent coupling*, *Phys. Rev.* **D66** (2002) 043503, [[hep-ph/0203242](#)].
- [27] K. Freese, P. Gondolo, H. J. Newberg, and M. Lewis, *The Effects of the Sagittarius Dwarf Tidal Stream on Dark Matter Detectors*, *Phys. Rev. Lett.* **92** (2004) 111301, [[astro-ph/0310334](#)]; R. Bernabei *et. al.*, *Investigating halo substructures with annual modulation signature*, *Eur. Phys. J.* **C47** (2006) 263–271, [[astro-ph/0604303](#)]; L. D. Duffy and P. Sikivie, *The Caustic Ring Model of the Milky Way Halo*, *Phys. Rev.* **D78** (2008) 063508, [[arXiv:0805.4556](#)].
- [28] T. Bruch, A. H. G. Peter, J. Read, L. Baudis, and G. Lake, *Dark Matter Disc Enhanced Neutrino Fluxes from the Sun and Earth*, *Phys. Lett.* **B674** (2009) 250–256, [[arXiv:0902.4001](#)].
- [29] K. Griest and D. Seckel, *Cosmic Asymmetry, Neutrinos and the Sun*, *Nucl. Phys.* **B283** (1987) 681.
- [30] A. Bottino, V. de Alfaro, N. Fornengo, G. Mignola, and M. Pignone, *On the neutralino as dark matter candidate. 1. Relic abundance*, *Astropart. Phys.* **2** (1994) 67–76, [[hep-ph/9309218](#)].
- [31] A. Bottino, F. Donato, N. Fornengo, and S. Scopel, *Implications for relic neutralinos of the theoretical uncertainties in the neutralino nucleon cross-section*, *Astropart. Phys.* **13** (2000) 215–225, [[hep-ph/9909228](#)]; A. Bottino, F. Donato, N. Fornengo, and S. Scopel, *Size of the neutralino nucleon cross-section in the light of a new determination of the pion nucleon sigma term*, *Astropart. Phys.* **18** (2002) 205–211, [[hep-ph/0111229](#)].
- [32] Other papers where the influence of the hadronic uncertainties on the neutralino-nuclei cross sections are discussed include: J. R. Ellis, A. Ferstl, and K. A. Olive, *Re-evaluation of the elastic scattering of supersymmetric dark matter*, *Phys. Lett.* **B481** (2000) 304–314, [[hep-ph/0001005](#)]; E. Accomando, R. L. Arnowitt, B. Dutta, and Y. Santoso, *Neutralino proton cross sections in supergravity models*, *Nucl. Phys.* **B585** (2000) 124–142, [[hep-ph/0001019](#)]; A. Corsetti and P. Nath, *Gaugino Mass Nonuniversality and Dark Matter in SUGRA, Strings and D Brane Models*, *Phys. Rev.* **D64** (2001) 125010, [[hep-ph/0003186](#)]; J. L. Feng, K. T. Matchev, and F. Wilczek, *Neutralino Dark Matter in Focus Point Supersymmetry*, *Phys. Lett.* **B482** (2000) 388–399, [[hep-ph/0004043](#)]; J. R. Ellis, K. A. Olive, and C. Savage, *Hadronic Uncertainties in the Elastic Scattering of Supersymmetric Dark Matter*, *Phys. Rev.* **D77** (2008) 065026, [[arXiv:0801.3656](#)]; J. Giedt, A. W. Thomas, and R. D. Young, *Dark matter, the CMSSM and lattice QCD*, [arXiv:0907.4177](#).
- [33] M. Cirelli *et. al.*, *Spectra of neutrinos from dark matter annihilations*, *Nucl. Phys.* **B727** (2005) 99–138, [[hep-ph/0506298](#)].

- [34] M. Blennow, J. Edsjo, and T. Ohlsson, *Neutrinos from WIMP Annihilations Using a Full Three- Flavor Monte Carlo*, *JCAP* **0801** (2008) 021, [[arXiv:0709.3898](#)].
- [35] V. Barger, W.-Y. Keung, G. Shaughnessy, and A. Tregre, *High energy neutrinos from neutralino annihilations in the Sun*, *Phys. Rev.* **D76** (2007) 095008, [[arXiv:0708.1325](#)]; J. Liu, P.-f. Yin, and S.-h. Zhu, *Neutrino Signals from Solar Neutralino Annihilations in Anomaly Mediated Supersymmetry Breaking Model*, *Phys. Rev.* **D77** (2008) 115014, [[arXiv:0803.2164](#)].
- [36] T. Schwetz, M. A. Tortola, and J. W. F. Valle, *Three-flavour neutrino oscillation update*, *New J. Phys.* **10** (2008) 113011, [[arXiv:0808.2016](#)].
- [37] T. K. Gaisser, *Cosmic Rays and Particle Physics*. Cambridge, UK: Cambridge University Press, Jan., 1991; T. K. Gaisser and T. Stanev, *Neutrino induced muon flux deep underground and search for neutrino oscillations*, *Phys. Rev.* **D30** (1984) 985; T. K. Gaisser and T. Stanev, *Response of deep detectors to extraterrestrial neutrinos*, *Phys. Rev.* **D31** (1985) 2770; N. Fornengo, *Neutrino oscillation effect on the indirect signal of neutralino dark matter from the earth core*, [hep-ph/9904351](#).
- [38] P. Lipari and M. Lusignoli, *Comparison of $\nu_\mu \leftrightarrow \nu_\tau$ and $\nu_\mu \leftrightarrow \nu_s$ oscillations as solutions of the atmospheric neutrino problem*, *Phys. Rev.* **D58** (1998) 073005, [[hep-ph/9803440](#)].
- [39] R. Abbasi *et al.*, *Limits on a muon flux from neutralino annihilations in the Sun with the IceCube 22-string detector*, *Phys. Rev. Lett.* **102** (2009) 201302, [[arXiv:0902.2460](#)].
- [40] E. Resconi and f. t. I. Collaboration, *Status and prospects of the IceCube neutrino telescope*, *Nucl. Instrum. Meth.* **A602** (2009) 7–13, [[arXiv:0807.3891](#)].
- [41] G. Wikstrom and J. Edsjo, *Limits on the WIMP-nucleon scattering cross-section from neutrino telescopes*, *JCAP* **0904** (2009) 009, [[arXiv:0903.2986](#)].
- [42] M. Honda, T. Kajita, K. Kasahara, and S. Midorikawa, *A new calculation of the atmospheric neutrino flux in a 3- dimensional scheme*, *Phys. Rev.* **D70** (2004) 043008, [[astro-ph/0404457](#)].
- [43] W. Lohmann, R. Kopp, and R. Voss, *Energy loss of muons in the energy range 1-GeV to 10000-GeV*, *CERN-85-03* (1985).
- [44] S. Desai *et al.*, *Search for dark matter WIMPs using upward through-going muons in Super-Kamiokande*, *Phys. Rev.* **D70** (2004) 083523, [[hep-ex/0404025](#)].
- [45] Y. Ashie *et al.*, *A measurement of atmospheric neutrino oscillation parameters by Super-Kamiokande I*, *Phys. Rev.* **D71** (2005) 112005, [[hep-ex/0501064](#)].

- [46] C. Saji, *Study of upward-going muons in Super-Kamiokande*. PhD thesis, Niigata University, Mar, 2002.
- [47] For a thorough overview of the recent activity in this field, see for instance the talks and contributions presented at the TAUP 2009 Conference (<http://taup2009.lngs.infn.it/prog.html>).
- [48] A. Bottino, N. Fornengo, G. Polesello, and S. Scopel, *Light neutralinos at CERN LHC in cosmologically-inspired scenarios: New benchmarks in the search for supersymmetry*, *Phys. Rev.* **D77** (2008) 115026, [[arXiv:0801.3334](https://arxiv.org/abs/0801.3334)]; A. Bottino, S. Choi, N. Fornengo, and S. Scopel (in preparation).

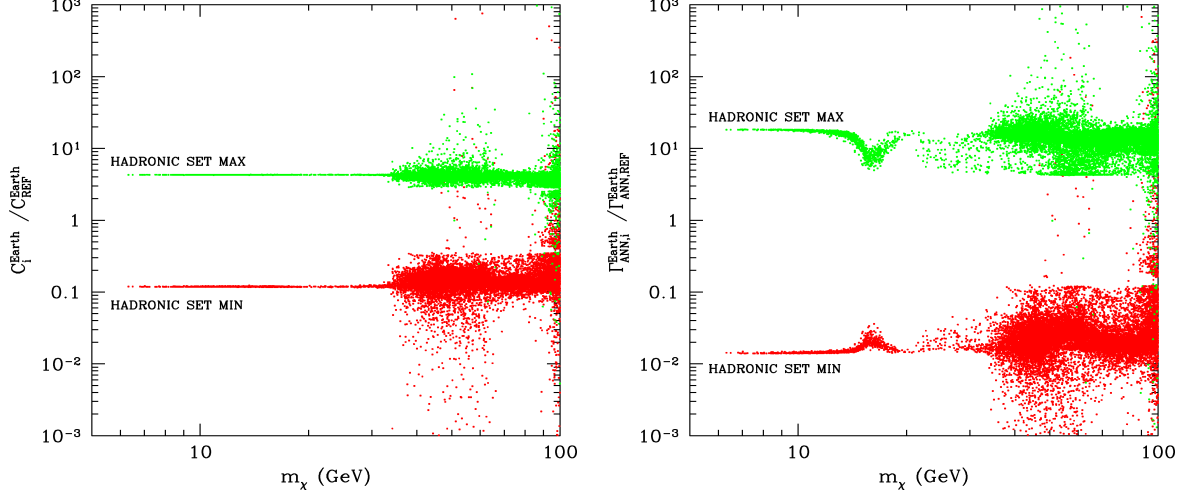


Figure 1: Ratios of capture rates (left panel) and annihilation rates (right panel), in the case of the Earth, calculated for the hadronic sets MIN and MAX with respect to the hadronic set REF. The local rotational velocity is set to its central value: $v_0 = 220 \text{ Km s}^{-1}$ ($\rho_0 = 0.34 \text{ GeV cm}^{-3}$).

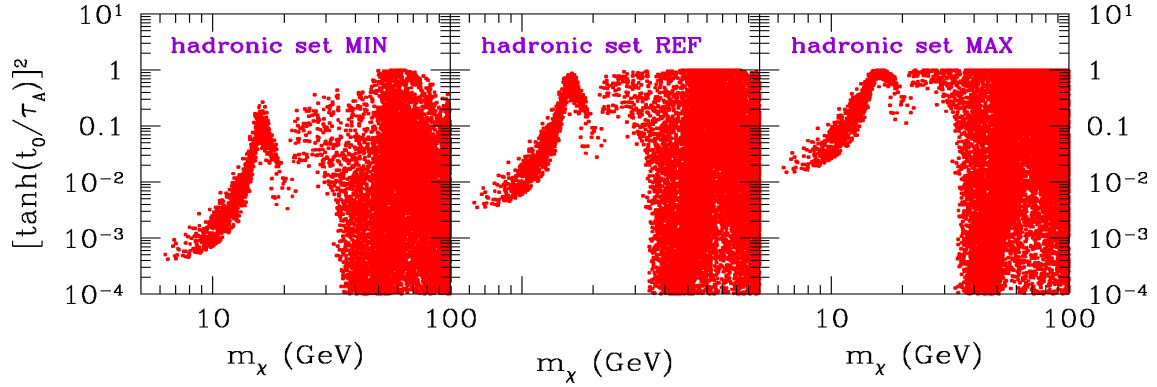


Figure 2: Equilibrium factor $\tanh^2(t_0/\tau_A)$, in the case of the Earth, displayed for the hadronic sets MIN, REF and MAX. The local rotational velocity is set to its central value: $v_0 = 220 \text{ Km s}^{-1}$ ($\rho_0 = 0.34 \text{ GeV cm}^{-3}$).

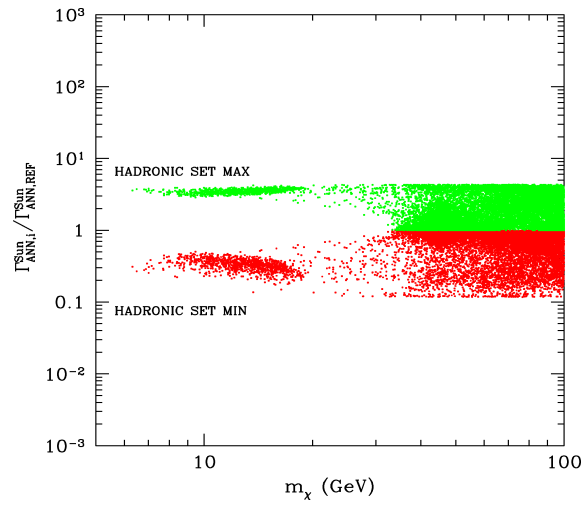


Figure 3: Ratios of annihilation rates, in the case of the Sun, calculated for the hadronic sets MIN and MAX with respect to the hadronic set REF. The local rotational velocity is set to its central value: $v_0 = 220 \text{ Km s}^{-1}$ ($\rho_0 = 0.34 \text{ GeV cm}^{-3}$).

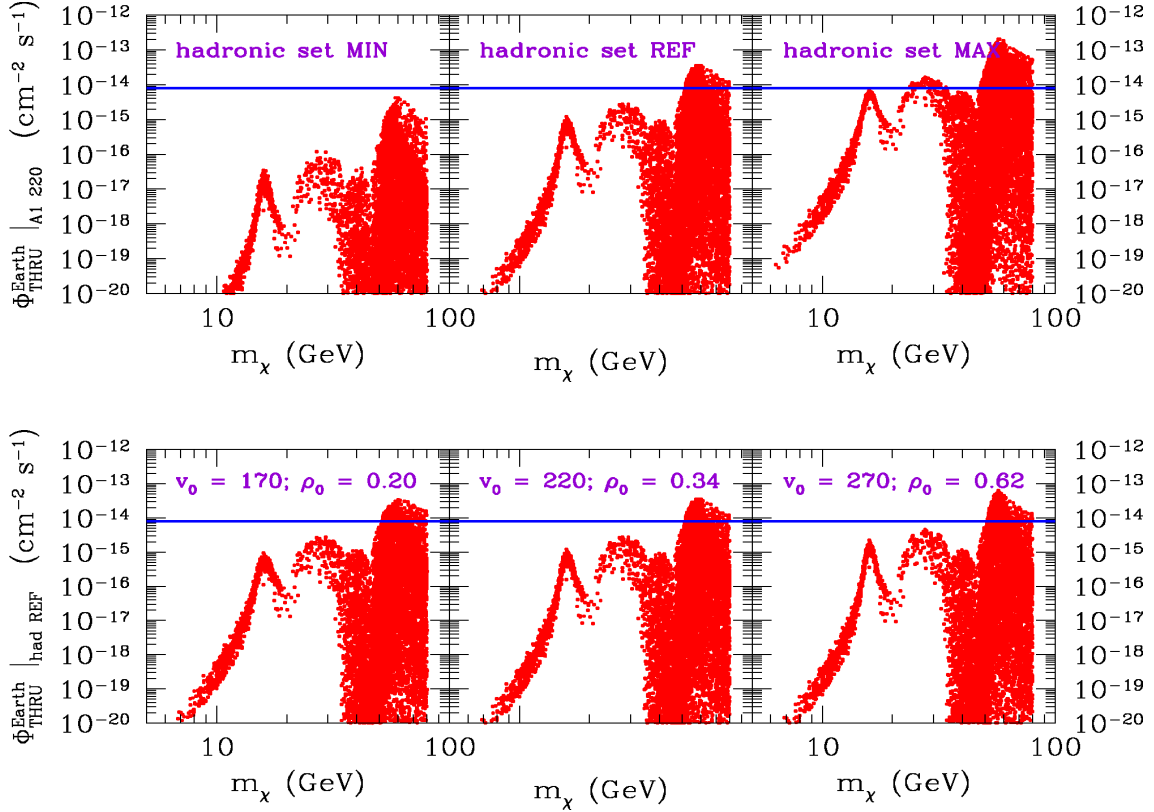


Figure 4: Upward through-going muon flux, generated by light neutralino pair-annihilation inside the Earth. The upper panel shows the dependence of the muon flux on the hadronic quantities, for fixed values of the astrophysical parameters: $v_0 = 220 \text{ Km s}^{-1}$ and $\rho_0 = 0.34 \text{ GeV cm}^{-3}$. The lower panel shows the dependence of the muon flux on the local rotational velocity v_0 and the total DM density ρ_0 , for the hadronic set REF. The horizontal line represents the experimental limit on through-going muons from the Earth obtained using the SK data, see Eq. (25).

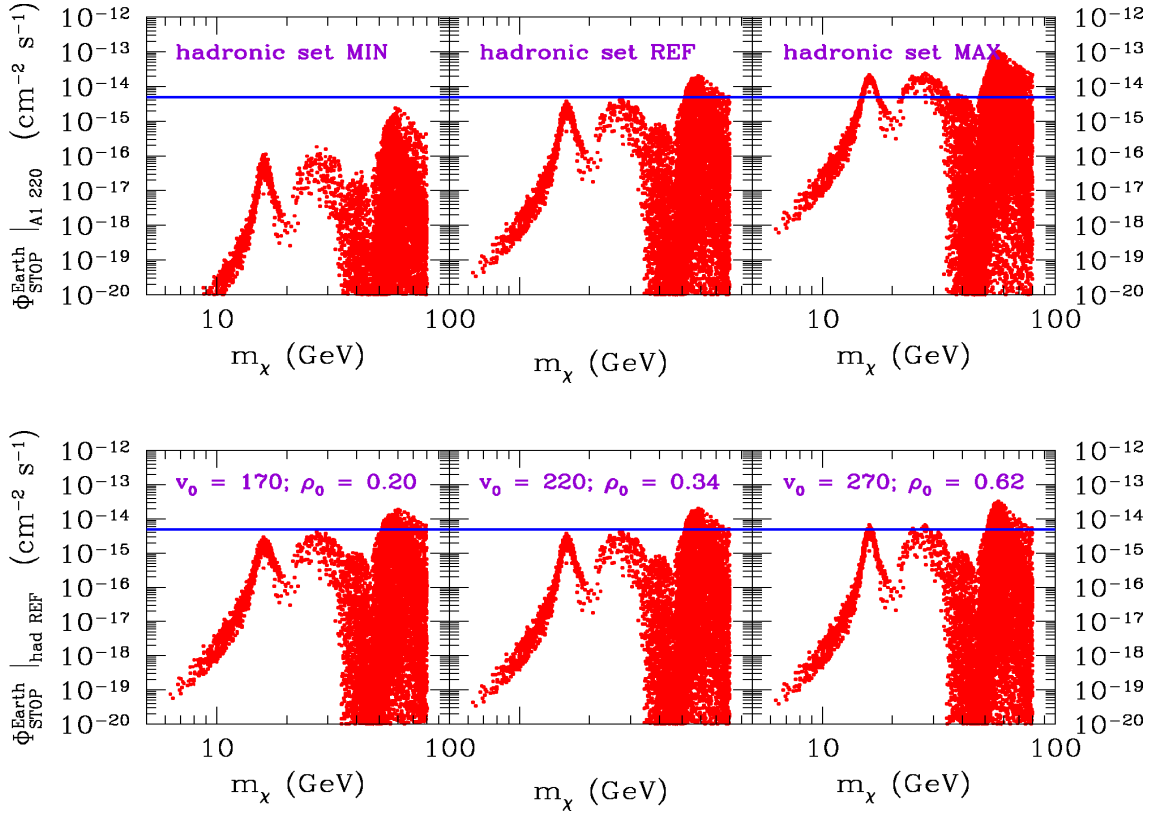


Figure 5: The same as Fig. 4, but in the case of upward stopping muons. In this case, the horizontal line refers to the experimental limit on stopping muons from the Earth obtained using the SK data, see Eq. (26).

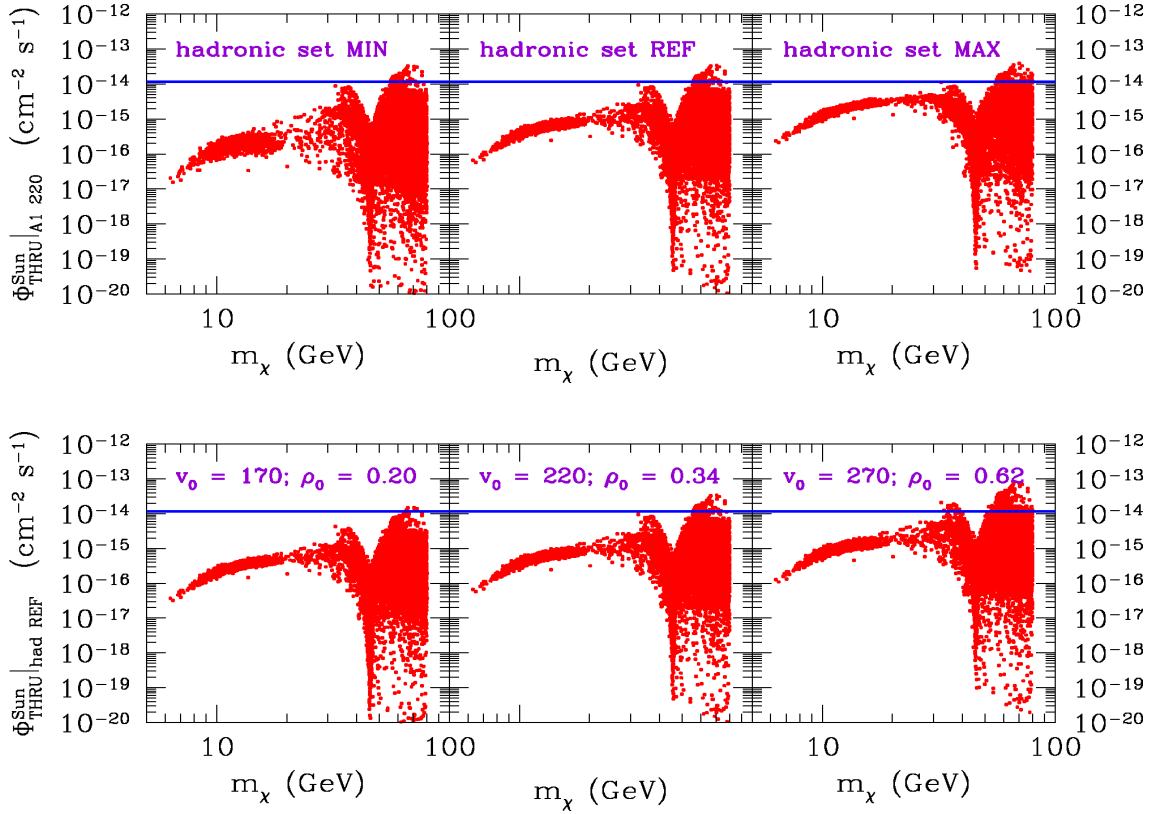


Figure 6: The same as Fig. 4, but in the case of light neutralino pair-annihilation inside the Sun. In this case, the horizontal line refers to the experimental limit on through-going muons from the Sun obtained using the SK data, see Eq. (27).

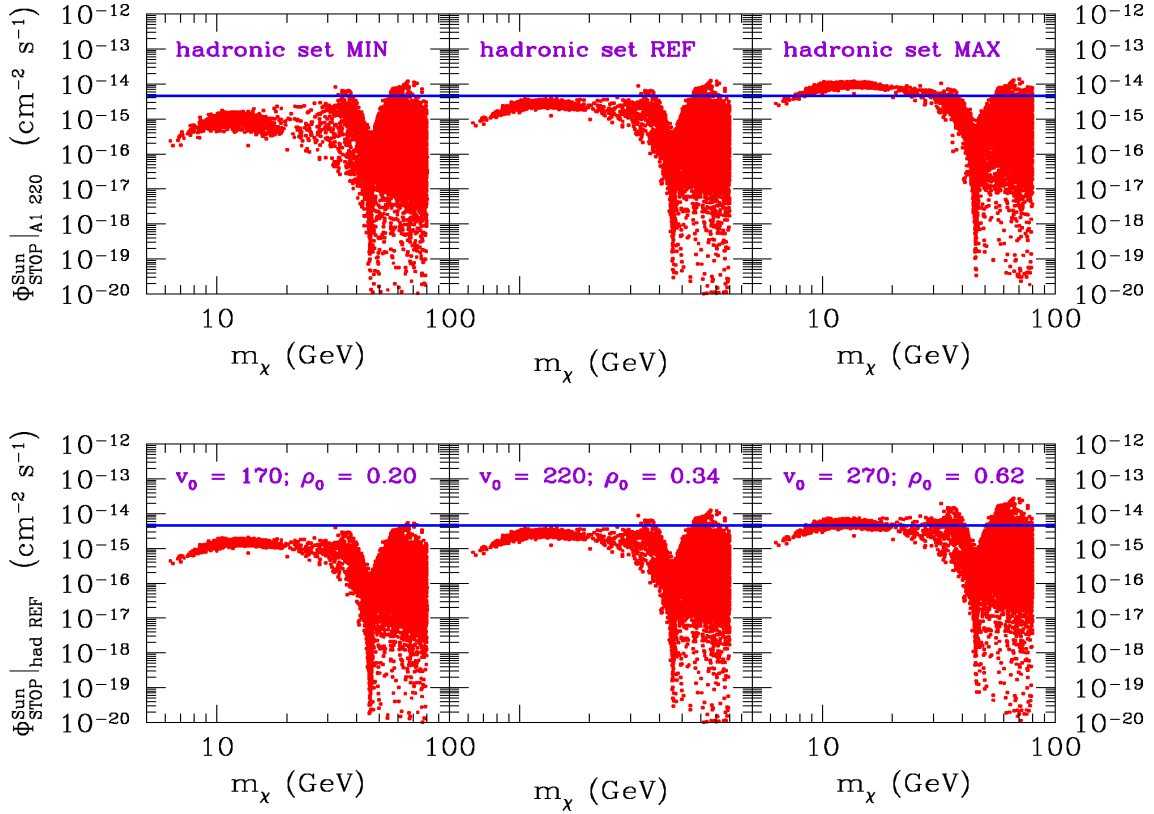


Figure 7: The same as Fig. 4, but in the case of light neutralino pair-annihilation inside the Sun and of upward stopping muons. In this case, the horizontal line refers to the experimental limit on stopping muons from the Sun obtained using the SK data, see Eq. (28).

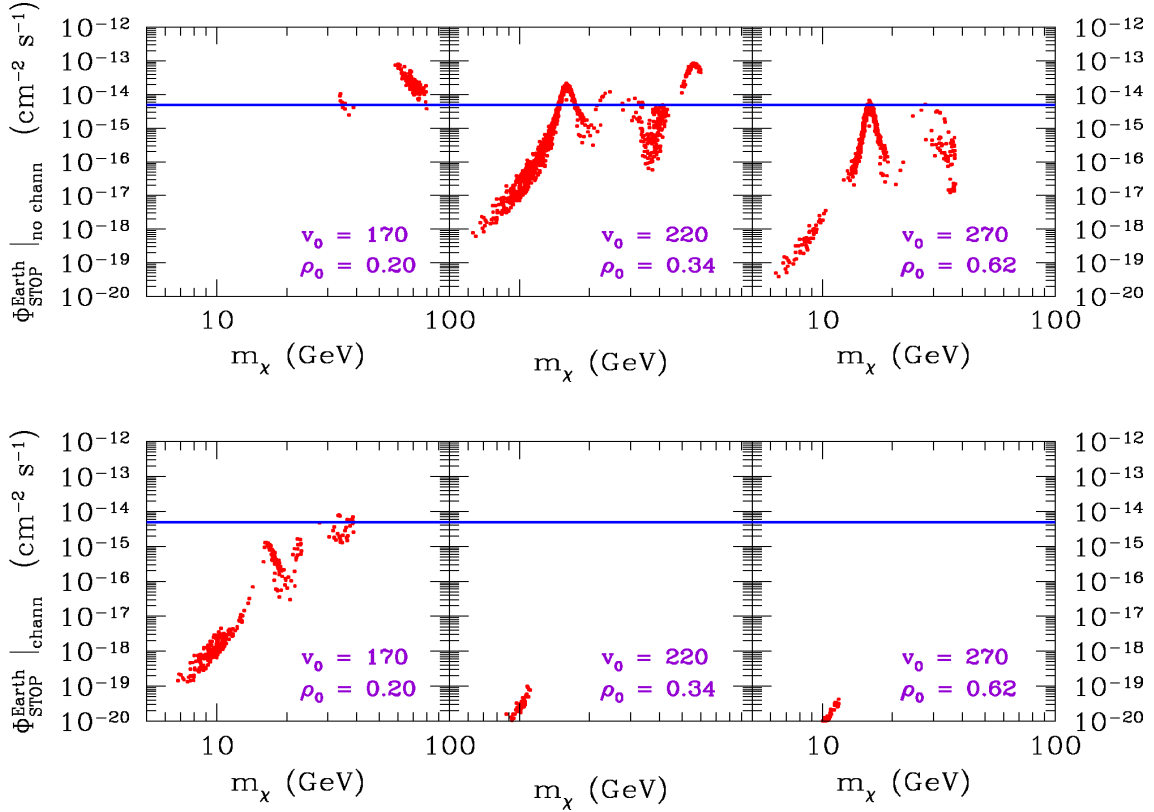


Figure 8: Upward stopping muon flux, generated by light neutralino pair-annihilation inside the Earth. The configurations displayed are only the ones compatible with the DAMA/LIBRA annual modulation region, obtained without including the channeling effect (upper panel) and including the channeling effect (lower panel). The three columns show the results for the different sets of astrophysical parameters, defined in Sect. 3. The set REF is used for the hadronic quantities. The horizontal line represents the experimental limit on stopping muons from the Earth obtained using the SK data, see Eq. (26).

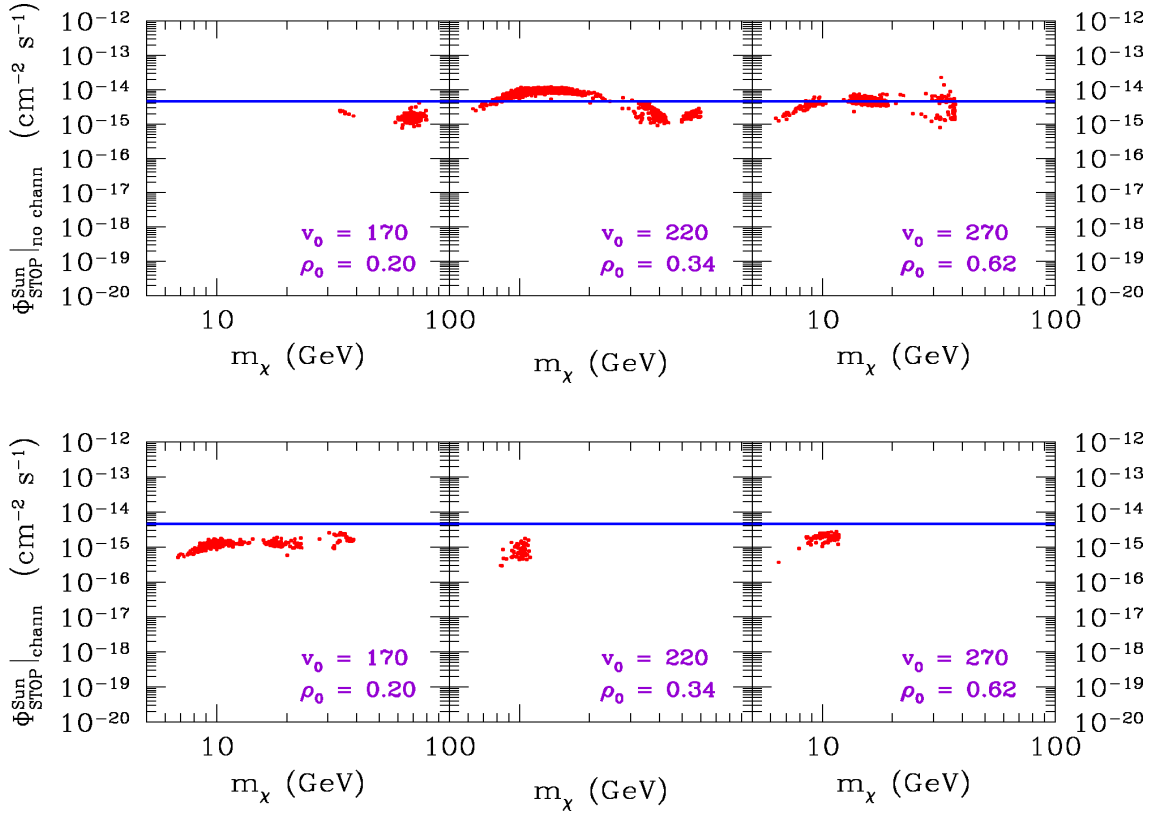


Figure 9: The same as Fig. 8, but in the case of light neutralino pair-annihilation inside the Sun. In this case, the horizontal line refers to the experimental limit on stopping muons from the Sun obtained using the SK data, see Eq. (28).